Original Article

Linear Accuracy and Reliability of Cone Beam CT Derived 3-Dimensional Images Constructed Using an Orthodontic Volumetric Rendering Program

Danielle R. Periago[a]; William C. Scarfe[b]; Mazyar Moshiri[c]; James P. Scheetz[d]; Anibal M. Silveira[e]; Allan G. Farman[f]

ABSTRACT

Objective: To compare accuracy of linear measurements made on cone beam computed tomographic (CBCT) derived 3-dimensional (3D) surface rendered volumetric images to direct measurements made on human skulls.

Materials and Methods: Twenty orthodontic linear measurements between anatomical landmarks on 23 human skulls were measured by observers using a digital caliper. The skulls were imaged with CBCT and Dolphin 3D (version 2.3) software used to generate 3D volumetric reconstructions (3DCBCT). The linear measurements between landmarks were computed by a single observer three times and compared to anatomic dimensions using Student's *t*-test ($P \leq .05$). The intraclass correlation coefficient (ICC) and absolute linear and percentage error were calculated.

Results: The ICC for 3DCBCT (0.975 $\pm$ 0.016) was significantly less than for skull (0.996 $\pm$ 0.007) measurements. Mean percentage measurement error for 3DCBCT (2.31% $\pm$ 2.11%) was significantly higher than replicate skull measurements (0.63% $\pm$ 0.51%). Statistical differences between 3DCBCT means and true dimensions were found for all of the midsagittal measurements except Na-A and six of the 12 bilateral measurements. The mean percentage difference between the mean skull and 3D-based linear measurements was -1.13% (SD $\pm$ 1.47%). Ninety percent of mean differences were less than 2 mm, and 95% confidence intervals were all less than 2 mm except for Ba-ANS (3.32 mm) and Pog-Go_{left} (2.42 mm).

Conclusions: While many linear measurements between cephalometric landmarks on 3D volumetric surface renderings obtained using Dolphin 3D software generated from CBCT datasets may be statistically significantly different from anatomic dimensions, most can be considered to be sufficiently clinically accurate for craniofacial analyses.

KEY WORDS: Computed tomography; Cone beam; Cephalometry; Diagnostic imaging; Head; 3D CT

[a] Graduate student (MS) and resident, Department of Orthodontic and Pediatric Dentistry, University of Louisville School of Dentistry, Louisville, Ky.

[b] Associate Professor, Department of Surgical/Hospital Dentistry, University of Louisville, Louisville, Ky.

[c] Graduate student (MS) and resident, Department of Orthodontic and Pediatric Dentistry, University of Louisville School of Dentistry, Louisville, Ky.

[d] Professor, Department of Diagnostic Sciences, Prosthetic and Restorative Dentistry, University of Louisville School of Dentistry, Louisville, Ky.

[e] Associate Professor, Department of Orthodontic and Pediatric Dentistry, University of Louisville School of Dentistry, Louisville, Ky.

[f] Professor, Department of Surgical/Hospital Dentistry, University of Louisville, Louisville, Ky.

Corresponding author: Dr William Charles Scarfe, Department of Surgical/Hospital Dentistry, University of Louisville, 501 South Preston St, Louisville, KY 40292
(e-mail: wcscar01@gwise.louisville.edu)

Accepted: May 2007. Submitted: December 2006.

INTRODUCTION

Recently, cone beam computed tomography (CBCT) systems have been developed specifically for the maxillofacial region.[1] Many devices are capable of a large field of view imaging of the skull to include most anthropometric landmarks used in cephalometric analysis. Time and dose requirements have been suggested to be of the same order of magnitude as other dental radiographic modalities.[2] Recently, maxillofacial applications of CBCT imaging have included craniofacial assessment in orthodontics.[3–5] High dimensional accuracy has been reported for maxillofacial CBCT in measurement of facial structures.[6–9]

CBCT derived 3D cephalometry has a number of potential advantages over conventional CT for cephalometric imaging including submillimeter resolution and reduced radiation exposure, while still permitting reconstruction of the soft tissue profile. Moreover, CBCT datasets can be imported as DICOM files into

Table 1. Definition of Linear Planes Used in the Cephalometric Analysis

Abbreviation	Name	Definition
Midsagittal Planes		
S-Na	Sella-nasion	A line connecting sella and nasion used to represent the cranial base in the midsagittal plane.
Na-Ba	Nasion-basion	A line connecting nasion and basion in the midsagittal plane used to represent the cranial base in the Ricketts analysis.
ANS-PNS	Anterior nasal spine-posterior nasal spine	A line connecting ANS and PNS. Used to represent the palatal plane or angle of the maxilla.
Na-A	Nasion-A point	A line connecting nasion and A point. A sagittal reference line for the maxilla's anterior-posterior position in the Steiner analysis.
Na-B	Nasion-B point	A line connecting nasion and B point. Represents the anterior-posterior position of the mandible in the Steiner analysis.
Na-Me	Nasion-menton	A line connecting nasion and menton. Represents total anterior face height.
Na-ANS	Nasion-anterior nasal spine	A line connecting nasion and ANS. Represents upper facial height.
Ba-ANS	Basion-anterior nasal spine	A line connecting basion and anterior nasal spine.
Bilateral Planes		
Pog-Go	Pogonion-gonion	A line connecting pogonion and gonion. Represents the length of the mandibular body.
Pog-Co	Pogonion-condylion	A line connecting pogonion and condylion. Represents mandibular unit length.
Go-Me	Gonion-menton	A line connecting gonion and menton. Represents the mandibular plane.
Go-Co	Gonion-condylion	A line connecting gonion and condylion. Represents posterior facial height.
Go-Gn	Gonion-gnathion	A line connecting gonion and gnathion. Used to represent the mandibular plane in the Steiner analysis.
Po-Or	Porion-orbitale	A line connecting porion and orbitale. Frankfort horizontal.

personal computer–based software to provide 3D reconstruction of the craniofacial skeleton. These possibilities and increasing access to CBCT imaging for orthodontics are enabling movement from 2D cephalometry to 3D visualization of craniofacial morphology.[10] However, there is a lack of data regarding the reliability and accuracy of linear measurements obtained from 3D volumetric renderings of CBCT data constructed from orthodontic software. Studies indicate that 3D reconstructions of conventional fan beam CT datasets have a high degree of accuracy[11–16] with differences between measured and actual dimensions being 2–3 mm.[17,18] Recently, methodological approaches to cephalometric analysis of 3D CT images have also been described.[19,20] We hypothesize that the accuracy of linear measurements obtained from 3D surface renderings of CBCT datasets is similar to the accuracy of measurements obtained from conventional CT datasets using orthodontic specific software.

Hence, the aim of the present study was to compare the reliability and accuracy of linear measurements made on 3D reconstructions generated using Dolphin 3D (Dolphin Imaging, Chatsworth, Calif) software applied to i-CAT (Imaging Sciences International, Hatfield, Pa) CBCT DICOM image datasets to direct measurements made on ex vivo human skulls.

MATERIALS AND METHODS

The investigation was an observational cross-sectional ex vivo experiment, approved by the Institutional Human Remains Committee, Department of Anatomical Sciences and Neurobiology at our university.

Twenty-three anonymous dry human skulls with a stable and reproducible occlusion and full permanent dentition were available. Fourteen craniometric anatomic landmarks were identified on each skull using an indelible marker according to currently accepted operational definitions.[21] Since it was not possible to locate coordinates in space, we defined Sella (S) to be the midpoint of rim between the anterior clinoid process in the median plane. The dimensions between specific points provided 20 linear distances commonly used in lateral cephalometric orthodontic analysis (Table 1). To minimize the inherent interrater differences in landmark identification and establish a fiducial anatomic location, the distance between each landmark was achieved by consensus of two observers (MM,

AB). Measurements were made three times by both observers independently using an electronic digital caliper (27-500-90, GAC, Bohemia, NY). The mean of the measurements was designated as the dimensional truth.

To provide some degree of soft-tissue equivalent attenuation, two latex balloons filled with water were placed in the cranial vault prior to imaging.[22] A 1.5-mm thick polystyrene foam wedge was placed in the joint space to separate the glenoid fossa and the condylar head. Prior to imaging, the dentition was placed in maximum intercuspation and the jaws held closed by bilateral metal springs. A custom plastic head holder was constructed to support the skulls during imaging.

Cone beam CT images were acquired using the i-CAT system. The skull was positioned according to manufacturer's instructions. Lateral scout radiographs were made and small adjustments to head position were made so that discrepancies between bilateral structures were less than 5 mm. A single 360° rotation, 20-second scan, comprising 306 basis projections was then made for each skull with a 17.0 cm (diameter) × 13.2 cm (height) field of view using XoranCat acquisition software (version 1.7.7, Xoran Technologies, Ann Arbor, Mich). Exposure parameters were controlled by automatic exposure control.

The CBCT data were exported from the XoranCat software in DICOM multi-file format and imported into Dolphin 3D (Prerelease version 2.3, Dolphin Imaging) on the same computer. All constructions and measurements were performed on a 20.1-inch flat panel color active matrix TFT screen (FlexScan L888, Eizo Nanao Technologies Inc, Cypress, Calif) with a resolution of 1600 × 1200 at 85 Hz and a 0.255 mm dot pitch, operated at 24 bit.

Three-dimensional reconstructions and measurements were undertaken in three stages:

— 3D surface rendering was generated by manually adjusting the threshold of visible pixel levels. This was the method used for segmentation (Figure 1).
— The cephalometric landmarks were located and marked on the 3D surface rendered volumetric image. The Dolphin 3D software provided various views using rotation and translation of the rendered image. Landmarks were identified by using a cursor-driven pointer. This was performed by a sequence of preset volumetric orientations (Figure 2). The volume was initially oriented in the posterior-anterior projection and Na, A point, ANS, B point, Gn, Pog and Or bilaterally located (Figure 2A). Next, the volume was oriented in the submento-vertex projection, and Me, PNS and Ba were identified (Figure 2B). Then the volume was rotated to the lateral projection and Co, Po and, Go located (Figure 2C and 2D.). Finally the volume was oriented to demonstrate the cranial fossa and S was located (Figure 2E). As the volume rendering was reoriented, the positions of the previously positioned landmarks were verified and, if necessary, relocated.
— Finally, measurements between specific landmarks were made. For the prerelease software version used, specific points and planes were unnamed. Therefore, it was necessary to select specific points to identify a linear plane. This was performed in a specific sequence such that linear measurement 1 corresponded to Na-A, linear measurement 2 corresponded to Na-B, and so forth. In this way the resulting analysis provided specific linear measurements (Figure 3) which could be exported as text data.

The version of the Dolphin 3D imaging software that was used in this investigation did not allow the user to "save" the location of the identified landmark on the 3D volumetric surface rendering, creating a digitally indelible landmark position. Therefore, for each of the three repeated measurements performed by the first author it was necessary to relocate landmarks and remeasure distances.

Statistical Analysis

A standard statistical software package (SPSS version 12, Chicago, Ill) was used for data analysis. To determine intraobserver reliability, the average measures intraclass correlation coefficient (ICC) was determined for repeat measurements. In addition, absolute and percentage mean error, standard deviations, and 95% confidence levels were calculated. Absolute and percentage linear means of triplicate measurements between specified anatomic landmarks were calculated and standard deviations and 95% confidence levels calculated. The digital measurements of the skulls were taken as a dimensional truth and compared with the 3D CBCT measurements with a 2-tailed paired Student's *t*-test at an à priori level of significance of $P \leq .05$.

RESULTS

The average measure ICC of triplicate skull measurements (0.996 ± 0.007; range: 0.981–0.991) was significantly higher than the mean ICC for 3D CBCT (0.976 ± 0.016; range: 0.941–0.993) ($t = 5.468$; $P < .001$) (Table 2).

The mean percentage measurement error for 3D CBCT (2.31% ± 2.11%; range: 1.07% ± 0 .72% to

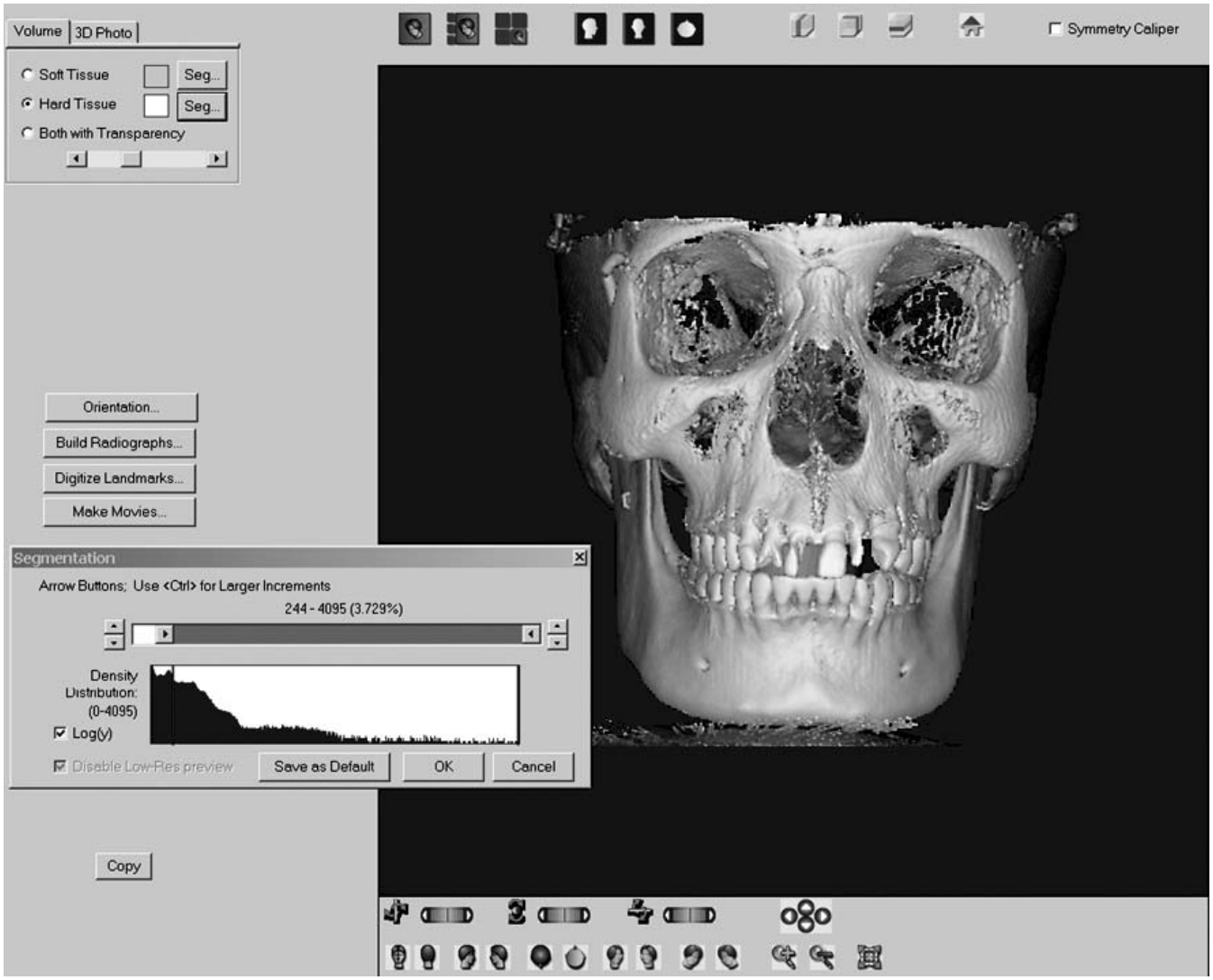

Figure 1. Image capture from Dolphin 3D program demonstrating the segmentation screen. The hard-tissue volume segmentation is selected (upper left) and using the segmentation cursor (lower left), the displayed gray level of the voxels is dynamically altered to provide the most realistic appearance of the skull with minimal loss of cortical bone due to thin structures and minimal superimposition of artifacts and soft tissue.

3.86% ± 1.85%) was significantly higher than repeated measurements to directly determine anatomic skull dimensions (0.63% ± 0.51%; range: 0.29% ± 0.13% to 1.18% ± 0.58%) ($t = 16.6$, $P < .001$) (Table 3). For all measurements except Ba-Na, 3D CBCT mean absolute and percentage error was significantly higher than direct skull repeated measurements.

The 3D CBCT data was found to have significant differences to actual skull measurements for 13 of the 20 parameters: seven of the eight midsagittal measurements (all except Na-A) and six of the 12 bilateral measurements (Pog-Go_{right}, Go-Me, Go-Gn_{left}, and Po-Or) (Table 4). The greatest mean difference of 3.32 mm (3.56%) was found with Ba-ANS. In eight of 20 measurements (40%) an average difference of less than 1 mm, three of which were significantly different from actual measurements, was found. In six measurements (30%) a mean difference between 1 mm and 1.5 mm was found, and for five skulls the CBCT measurements were significantly different from actual measurements made directly on the anatomic specimens. In four measurements (20%) an average difference of 1.5 mm to 2 mm was found, all of which were significantly different from the assumed anatomic truth. Finally, for two measurements (10%) a mean difference greater than 2 mm was found, one of which was significantly different from the mean direct skull measurements. In all comparisons, except Na-B and Go-Gn bilaterally, 3D CBCT measurements were less than skull measurements. The mean percentage difference between the mean skull and 3D-based linear measurements was −1.13% (SD ± 1.47%) and

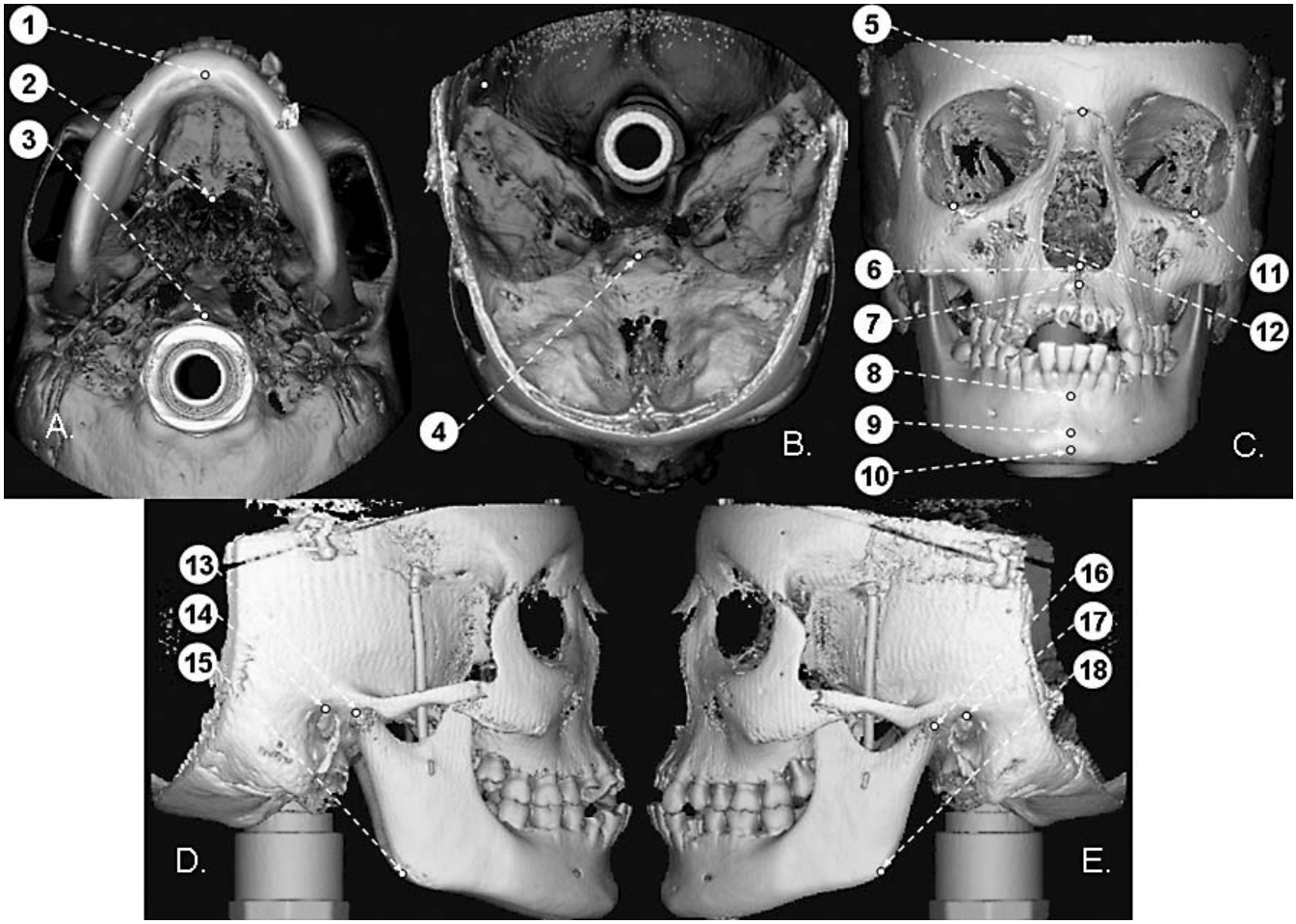

Figure 2. Volumetric surface rendered projections derived from Dolphin 3D showing anatomic landmark identification sequence: (A) Inferior projection: 1, menton; 2, PNS; 3, basion. (B) Superior projection: 4, sella. (C) Frontal projection: 5, nasion; 6, ANS; 7, A point; 8, B point; 9, pogonion; 10, gnathion; 11, left orbitale; 12, right orbitale. (D) Right lateral projection: 13, right condylion; 14, right porion; 15, right gonion. (E) Left lateral projection: 16, left condylion; 17, left porion; 18, left gonion.

ranged from −0.27% for Na-A to −3.44% for ANS-PNS.

DISCUSSION

The introduction of maxillofacial CBCT equipment provides clinicians with an opportunity to generate 3D volumetric renderings easily using relatively inexpensive third-party personal computer–based software. The rapidly emerging availability of this technology will undoubtedly expand the use and application of 3D imaging, particularly in the field of orthodontics.[23–26] The aim of this study was to compare the reliability and accuracy of linear measurements made on 3D volumetric reconstructions generated from CBCT datasets using a proprietary orthodontic image and analysis program to direct measurements made on ex vivo human skulls.

It was found that for two-thirds of dimensions, CBCT measurements were statistically significantly different from actual measurements. However, analyzing the absolute and percentage differences, this statistical significance probably does not translate into clinical relevance. Statistical differences most likely resulted

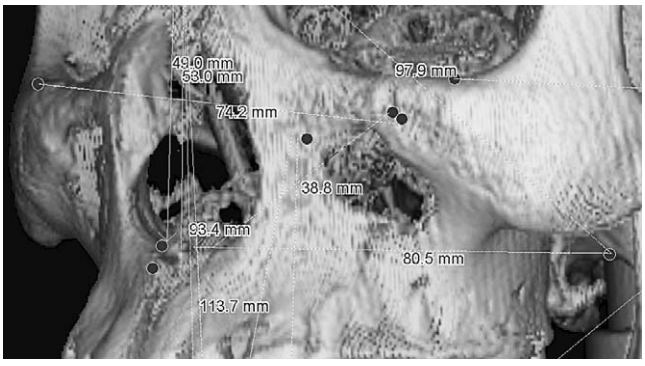

Figure 3. Cropped surface rendered 3D image of the midfacial region generated from segmentation demonstrating location of some of the landmarks and linear dimensions measured in the study.

Table 2. Average Measure Intraclass Correlation Coefficient for Triplicate Measurements for Midsagittal and Bilateral Linear Measurements by Multiple Observers on 23 Skulls and for a Single Observer on CBCT 3D Reconstructions

		Modality					
		Skull			CBCT 3D Reconstructions		
			95% Confidence Interval			95% Confidence Interval	
Plane	Location	Mean	Lower	Upper	Mean	Lower	Upper
S-N	Midsagittal	0.998	0.996	0.999	0.941	0.882	0.973
Ba-Na	Midsagittal	0.996	0.994	0.998	0.993	0.987	0.997
ANS-PNS	Midsagittal	0.994	0.989	0.997	0.954	0.907	0.979
Na-A	Midsagittal	0.999	0.997	0.999	0.964	0.928	0.983
Na-B	Midsagittal	0.996	0.994	0.998	0.964	0.927	0.983
Na-Me	Midsagittal	0.997	0.995	0.999	0.994	0.988	0.997
Na-ANS	Midsagittal	0.997	0.995	0.999	0.958	0.917	0.981
Ba-ANS	Midsagittal	0.990	0.981	0.996	0.979	0.957	0.990
Pog-Go	Right	0.999	0.999	0.999	0.987	0.974	0.994
	Left	0.999	0.999	0.999	0.990	0.980	0.995
Pog-Co	Right	0.999	0.999	0.999	0.952	0.904	0.978
	Left	0.969	0.998	0.999	0.972	0.944	0.987
Go-Me	Right	0.999	0.999	0.999	0.982	0.964	0.992
	Left	0.999	0.999	0.999	0.987	0.974	0.994
Go-Co	Right	0.999	0.998	0.999	0.990	0.981	0.996
	Left	0.999	0.999	0.999	0.983	0.966	0.992
Go-Gn	Right	0.997	0.993	0.999	0.965	0.931	0.984
	Left	0.995	0.990	0.998	0.986	0.972	0.994
Po-Or	Right	0.996	0.994	0.998	0.980	0.960	0.991
	Left	0.996	0.992	0.998	0.987	0.974	0.994

Table 3. Comparison of Absolute and Percentage Mean Error for Midsagittal and Bilateral Linear Measurements Between Dimensions of Planes on 23 Skulls and Measurements on CBCT 3D Reconstructions

		Skull				CBCT 3D Reconstructions					
		Absolute Error, mm		Percentage Error, %		Absolute Error, mm		Percentage Error, %		Significance	
Plane	Location[a]	Mean ± SD	95% Confidence Interval	Mean ± SD	95% Confidence Interval	Mean ± SD	95% Confidence Interval	Mean ± SD	95% Confidence Interval	*t*	*P*
S-N	MS	0.41 ± 0.20	0.09	0.7 ± 0.34	0.15	1.82 ± 0.86	0.37	3.86 ± 1.85	0.80	7.61	<.001
Ba-Na	MS	0.69 ± 0.35	0.15	0.70 ± 0.36	0.15	0.85 ± 0.60	0.26	1.07 ± 0.72	0.31	1.1	.280
ANS-PNS	MS	0.55 ± 0.25	0.11	1.18 ± 0.58	0.25	1.30 ± 1.46	0.63	3.55 ± 4.00	1.73	2.43	.019
Na-A	MS	0.33 ± 0.16	0.07	0.64 ± 0.31	0.13	1.44 ± 1.08	0.47	3.52 ± 2.62	1.13	4.90	<.001
Na-B	MS	0.33 ± 0.18	0.08	0.38 ± 0.20	0.09	1.41 ± 2.02	0.87	1.96 ± 2.76	1.19	2.53	.015
Na-Me	MS	0.49 ± 0.64	0.28	0.45 ± 0.54	0.23	1.05 ± 0.55	0.24	1.22 ± 0.65	0.28	3.16	<.01
Na-ANS	MS	0.32 ± 0.17	0.08	0.70 ± 0.36	0.16	1.16 ± 0.86	0.37	3.20 ± 2.45	1.06	4.54	<.001
Ba-ANS	MS	1.07 ± 0.93	0.40	1.16 ± 0.99	0.43	2.11 ± 2.12	0.91	2.98 ± 3.13	1.35	2.15	.040
Pog-Go	Rt	0.29 ± 0.10	0.05	0.35 ± 0.13	0.06	1.24 ± 1.12	0.48	1.88 ± 1.77	0.76	4.04	<.001
	Lt	0.30 ± 0.11	0.05	0.36 ± 0.13	0.06	1.21 ± 0.80	0.34	1.83 ± 1.14	0.49	5.40	<.001
Pog-Co	Rt	0.33 ± 0.15	0.06	0.29 ± 0.13	0.06	2.27 ± 1.80	0.78	2.49 ± 2.05	0.89	5.16	<.001
	Lt	0.35 ± 0.24	0.10	0.31 ± 0.21	0.09	1.61 ± 1.65	0.72	1.77 ± 1.91	0.83	3.60	<.001
Go-Me	Rt	0.31 ± 0.15	0.06	0.38 ± 0.19	0.08	1.33 ± 0.86	0.37	2.12 ± 1.31	0.56	5.66	<.001
	Lt	0.40 ± 0.59	0.25	0.51 ± 0.75	0.33	1.11 ± 0.90	0.39	1.77 ± 1.38	0.60	3.17	<.01
Go-Co	Rt	0.37 ± 0.18	0.08	0.65 ± 0.30	0.13	0.97 ± 0.71	0.31	2.13 ± 1.50	0.65	3.91	<.001
	Lt	0.30 ± 0.12	0.05	0.54 ± 0.23	0.10	1.12 ± 0.97	0.42	2.45 ± 2.03	0.78	4.04	<.001
Go-Gn	Rt	0.69 ± 0.51	0.22	0.88 ± 0.68	0.29	1.56 ± 1.24	0.54	2.44 ± 1.98	0.86	3.08	<.01
	Lt	0.71 ± 0.66	0.29	0.88 ± 0.78	0.34	1.43 ± 0.77	0.33	2.22 ± 1.28	0.55	3.36	<.01
Po-Or	Right	0.56 ± 0.23	0.10	0.70 ± 0.28	0.12	1.22 ± 0.90	0.39	1.96 ± 1.45	0.63	3.41	<.01
	Left	0.58 ± 0.18	0.08	0.74 ± 0.23	0.10	1.10 ± 0.68	0.29	1.80 ± 1.13	0.49	3.54	<.001

[a] MS indicates midsagittal; Rt, right; Lt, left.

Table 4. Comparison of Absolute and Percentage Differences for Midsagittal and Bilateral Linear Measurements Between Dimensions of Planes on 23 Skulls and Measurements on CBCT 3D Reconstructions

				Difference					
				Absolute		Percentage		Significance	
Plane	Location[a]	Skull	CBCT 3D Reconstructions	Mean	95% Confidence Interval	Mean	95% Confidence Interval	*t*	*P*
S-N	MS	59.31 ± 3.75	58.56 ± 3.67	−0.75	(−1.25 to −0.24)	−1.26	(−2.11 to −0.4)	−3.059	.006
Ba-Na	MS	98.81 ± 4.99	97.18 ± 4.92	−1.63	(−2.02 to −1.25)	−1.65	(−2.04 to −1.27)	−8.72	<.001
ANS-PNS	MS	47.70 ± 3.25	46.06 ± 3.29	−1.64	(−2.32 to −0.95)	−3.44	(−4.86 to −1.99)	−4.94	<.001
Na-A	MS	51.00 ± 3.36	50.86 ± 3.23	−0.14	(−0.63 to 0.34)	−0.27	(−1.24 to 0.67)	−0.61	.546
Na-B	MS	88.64 ± 5.71	89.75 ± 6.07	1.11	(0.59 to 1.62)	1.25	(0.67 to 1.83)	4.5	<.001
Na-Me	MS	108.58 ± 7.06	107.77 ± 7.03	−0.81	(−1.26 to −0.36)	−0.75	(−1.16 to −0.33)	−3.77	.001
Na-ANS	MS	46.41 ± 2.86	45.58 ± 2.85	−0.83	(−1.10 to −0.55)	−1.79	(−2.37 to −1.19)	−6.17	<.001
Ba-ANS	MS	93.17 ± 6.31	89.85 ± 7.40	−3.32	(−4.96 to −1.68)	−3.56	(−5.32 to −1.8)	−4.19	<.001
Pog-Go	Rt	83.33 ± 5.83	81.86 ± 5.65	−1.48	(−2.08 to −0.87)	−1.78	(−2.50 to −1.04)	−5.09	<.001
	Lt	84.20 ± 9.76	81.78 ± 5.71	−2.42	(−5.31 to 0.47)	−2.87	(−6.31 to 0.56)	−1.73	.097
Pog-Co	Rt	114.77 ± 5.39	114.20 ± 4.84	−0.57	(−1.32 to 0.17)	−0.50	(−1.15 to 0.15)	−1.59	.127
	Lt	114.63 ± 5.44	113.88 ± 5.02	−0.75	(−1.67 to 0.16)	−0.65	(−1.46 to 0.14)	−1.69	.104
Go-Me	Rt	79.89 ± 5.59	78.16 ± 5.19	−1.73	(−2.35 to −1.12)	−2.17	(−2.94 to −1.4)	−5.83	<.001
	Lt	79.31 ± 5.93	78.21 ± 5.29	−1.09	(−1.64 to −0.55)	−1.37	(−2.07 to −0.69)	−4.14	<.001
Go-Co	Rt	56.38 ± 4.97	56.22 ± 4.71	−0.16	(−0.74 to 0.43)	−0.28	(−1.31 to 0.76)	−0.547	.590
	Lt	56.54 ± 5.04	56.00 ± 4.21	−0.53	(−1.07 to 0.002)	−0.94	(−1.89 to 0.0)	−2.067	.051
Go-Gn	Rt	79.85 ± 6.52	81.18 ± 6.02	1.33	(−0.064 to 2.72)	1.67	(−0.08 to 3.41)	1.98	.061
	Lt	79.78 ± 6.20	81.04 ± 5.92	1.27	(0.38 to 2.16)	1.59	(0.48 to 2.71)	2.95	.007
Po-Or	Right	78.97 ± 4.79	77.59 ± 4.43	−1.38	(−2.06 to −0.69)	−1.75	(−2.61 to −0.87)	−4.16	<.001
	Left	78.00 ± 4.82	76.33 ± 4.83	−1.67	(−2.41 to −0.93)	−2.14	(−3.09 to −1.19)	−4.68	<.001

[a] MS indicates midsagittal; Rt, right; Lt, left.

from small standard deviations within the measurements. In addition, the greater intraobserver variability demonstrated by the 3D CBCT measurements also may have so contributed.

These results are very similar in magnitude to those of Cavalcanti et al.[15] However, they reported no statistically significant difference between imaging and physical measurements. Their mean difference between actual and 3D-based linear measurements was 0.83% as compared with −1.13 ± 1.47% in the present study. In the present study, 40% of measurements had an average difference of less than 1 mm, 70% had an average difference of less than 1.5 mm, and 90% had an average difference of less than 2 mm. These absolute differences compare favorably with those reported by additional authors.[16,18]

There are numerous factors which should be considered when applying the results of this investigation to clinical situations. First and foremost, this study was performed on human skulls. The accuracy of measurement distances between three-dimensional landmarks on 3D volumes of patients may be affected by a reduction in image quality due to soft-tissue attenuation, metallic artifacts, and patient motion. Variation in scanning protocol such as voxel size and number of basis projection images may also influence measurement accuracy. Therefore, it would be expected that the dimensional accuracy of 3D measurements would be somewhat less on patient derived data.

There are also some potential limitations when using 3D images derived from CBCT data.[39] Three-dimensional volumetric depiction depends on appropriate segmentation—the thresholding of bone pixel values and suppression of surrounding tissue values to enhance the structure of interest. This process is dependent on the software algorithm, the spatial and contrast resolution of the scan, the thickness and degree of calcification or cortication of the bony structure, and the technical skill of the operator. In this study, the Dolphin 3D software provides a semimanual method of segmentation, dependent on the interaction of the operator with the data to produce a visually acceptable 3D rendering. These limitations result in deficiencies or voids in the surface of the image. These occur in regions that are represented by few voxels or have gray values still representing bone, but outside the threshold. These areas include the posterior and anterior superior walls of the maxillary sinus, bone overlying the dentition and cortical bone of the mandibular condyle. Consequently, this may lead to greater landmark identification error and subsequent measurement error. Anatomic landmarks whose accuracy may be affected by poor segmentation include A point, ANS, PNS, porion, and condylion.

In addition, the method of establishing dimensional truth could have potentially contributed to bias in the results. While the landmark identification and measurements on the 3D rendered images were repeated three times by a single observer, the landmark identification on the skulls was performed only once and

measurements performed three times by two observers independently. This reduced the error of point identification on the skulls. However, the establishment of a consensus landmark location was necessary to provide a fiducial reference to which we could assess the inherent clinical inaccuracies of both landmark identification and measurement associated with the 3D image rendering.

We were unable to completely simulate soft tissue effects of attenuation on image quality in this study as this would have been problematic in positioning and orientation of the skulls. While the use of water balloons placed within the cranial cavity provided some degree of soft-tissue attenuation, the lack of peripheral attenuation material may have allowed easier identification of landmarks on 3D surface rendered images.

In this study it was also found that mean intrarater error was significantly greater for almost all 3D CBCT measurements compared to actual skull measurements. This was most likely due to the differences in which landmarks were identified between the skull and volumetric image. Previous authors have used metallic markers as fiducial points on skulls to identify landmarks with subsequent images providing radiopaque landmarks. This methodology was not followed for the present investigation because of the desire to establish a control linear dimension on the skulls.

CONCLUSIONS

- While many linear measurements between cephalometric landmarks on 3D volumetric surface renderings obtained using Dolphin 3D software generated from i-CAT CBCT datasets may be statistically significantly different from anatomic dimensions, most can be considered to be sufficiently clinically accurate ($-1.13\% \pm 1.47\%$) for craniofacial analyses.

ACKNOWLEDGMENT

The authors wish to thank Ms April Brown, 2005 summer research associate and graduate student candidate for the Masters in Oral Biology at The University of Louisville School of Dentistry, for her valuable assistance in this project.

REFERENCES

1. Sukovic P. Cone beam computed tomography in craniofacial imaging. *Orthod Craniofac Res.* 2003;6(suppl 1):31–36.
2. Ludlow JB, Davies-Ludlow LE, Brooks SL, Howerton WB. Dosimetry of 3 CBCT devices for oral and maxillofacial radiology: CB Mercuray, NewTom 3G and i-CAT. *Dentomaxillofac Radiol.* 2006;35:219–226.
3. Maki K, Inou N, Takanishi A, Miller AJ. Computer-assisted simulations in orthodontic diagnosis and the application of a new cone beam X-ray computed tomography. *Orthod Craniofac Res.* 2003;6(suppl 1):95–101.
4. Aboudara CA, Hatcher D, Nielsen IL, Miller A. A three-dimensional evaluation of the upper airway in adolescents. *Orthod Craniofac Res.* 2003;6(suppl 1):173–175.
5. Danforth RA, Dus I, Mah J. 3-D volume imaging for dentistry: a new dimension. *J Calif Dent Assoc.* 2003;31:817–823.
6. Kobayashi K, Shimoda S, Nakagawa Y, Yamamoto A. Accuracy in measurement of distance using limited cone-beam computerized tomography. *Int J Oral Maxillofac Implants.* 2004;19:228–231.
7. Lascala CA, Panella J, Marques MM. Analysis of the accuracy of linear measurements obtained by cone beam computed tomography (CBCT-NewTom). *Dentomaxillofac Radiol.* 2004;33:291–294.
8. Beason R, Brooks SL. TMJ imaging accuracy using alpha prototype of DentoCAT™ cone-beam CT [abstract]. *J Dent Res.* 2004;83(special issue A):1938
9. Hilgers ML, Scarfe WC, Scheetz JP, Farman AG. Accuracy of linear TMJ measurements with cone beam computed tomography and digital cephalometric radiography. *Am J Orthod Dentofacial Orthop.* 2005;1278:803–811.
10. Swennen GRJ, Schutyser F. Three-dimensional cephalometry: spiral multi-slice vs cone-beam computed tomography. *Am J Orthod Dentofacial Orthop.* 2006;130:410–416.
11. Hildebolt CF, Vannier MW, Knapp RH. Validation study of skull three-dimensional computerized tomography measurements. *Am J Phys Anthropol.* 1990;82:283–294.
12. Kragskov J, Bosch C, Gyldensted C, Sindet-Pedersen S. Comparison of the reliability of craniofacial anatomic landmarks based on cephalometric radiographs and three-dimensional CT scans. *Cleft Palate Craniofac J.* 1997;34:111–116.
13. Nagashima M, Inoue K, Sasaki T, Miyasaka K, Matsumura G, Kodama G. Three-dimensional imaging and osteometry of adult human skulls using helical computed tomography. *Surg Radiol Anat.* 1998;20:291–297.
14. Cavalcanti MG, Rocha SS, Vannier MW. Craniofacial measurements based on 3D-CT volume rendering: implications for clinical applications. *Dentomaxillofac Radiol.* 2004;33:170–176.
15. Cavalcanti MG, Vannier MW. Quantitative analysis of spiral computed tomography for craniofacial clinical applications. *Dentomaxillofac Radiol.* 1998;27:344–350.
16. Jung H, Kim HJ, Kim DO, et al. Quantitative analysis of three-dimensional rendered imaging of the human skull acquired from multi-detector row computed tomography. *J Digit Imaging.* 2002;15:232–239.
17. Cavalcanti MG, Haller JW, Vannier MW. Three-dimensional computed tomography landmark measurement in craniofacial surgical planning: experimental validation in vitro. *J Oral Maxillofac Surg.* 1999;57:690–694.
18. Williams FL, Richtsmeier JT. Comparison of mandibular landmarks from computed tomography and 3D digitizer data. *Clin Anat.* 2003;16:494–500.
19. Park SH, Yu HS, Kim KD, Lee KJ, Baik HS. A proposal for a new analysis of craniofacial morphology by 3-dimensional computed tomography. Am J Orthod Dentofacial Orthop. 2006;129:600.e23–e34.
20. Maeda M, Katsumata A, Ariji Y, Muramatsu A, Yoshida K, Goto S, Kurita K, Ariji E. 3D-CT evaluation of facial asymmetry in patients with maxillofacial deformities. *Oral Surg Oral Med Oral Pathol Oral Radiol Endod.* 2006;102:382–390.
21. Caufield PW. Tracing technique and identification of land-

marks. In: Jacobson A, Jacobson RL, eds. *Radiographic Cephalometry: From Basics to 3-D Imaging.* 2nd ed. Hanover Park, IL: Quintessence; 2006:45–51.
22. Moshiri M, Scarfe WC, Hilgers ML, Scheetz JP, Silveira AM, Farman AG. Accuracy of linear measurements from imaging plate and CBCT-derived lateral cephalometric images. *Am J Orthod Dentofacial Orthop.* In press.
23. Danforth RA, Dus I, Mah J. 3-D volume imaging for dentistry: a new dimension. *J Calif Dent Assoc.* 2003;31:817–823.
24. Kau CH, Richmond S, Palomo JM, Hans MG. Three-dimensional cone beam computerized tomography in orthodontics. *J Orthod.* 2005;32:282–293.
25. Cevidanes LH, Styner MA, Proffit WR. Image analysis and superimposition of 3-dimensional cone-beam computed tomography models. *Am J Orthod Dentofacial Orthop.* 2006; 129:611–618.
26. Weinberg SM, Kolar JC. Three-dimensional surface imaging: limitations and considerations from the anthropometric perspective. *J Craniofac Surg.* 2005;16:847–851.